A LETTERS JOURNAL EXPLORING THE FRONTIERS OF PHYSICS

OFFPRINT

Different water scenarios for a primitive model with two types of hydrogen bonds

YUSONG TU, SERGEY V. BULDYREV, ZENGRONG LIU, HAIPING FANG and H. EUGENE STANLEY

EPL, **97** (2012) 56005

epl

A Letters Journal Exploring the Frontiers of Physics

AN INVITATION TO SUBMIT YOUR WORK

www.epljournal.org

The Editorial Board invites you to submit your letters to EPL

EPL is a leading international journal publishing original, high-quality Letters in all areas of physics, ranging from condensed matter topics and interdisciplinary research to astrophysics, geophysics, plasma and fusion sciences, including those with application potential.

The high profile of the journal combined with the excellent scientific quality of the articles continue to ensure EPL is an essential resource for its worldwide audience. EPL offers authors global visibility and a great opportunity to share their work with others across the whole of the physics community.

Run by active scientists, for scientists

EPL is reviewed by scientists for scientists, to serve and support the international scientific community. The Editorial Board is a team of active research scientists with an expert understanding of the needs of both authors and researchers.

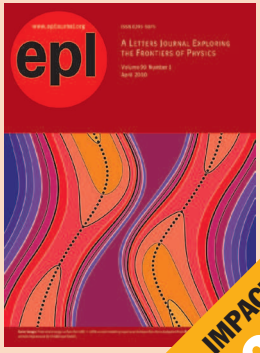

IMPACT FACTOR 2.753*

*As ranked by ISI 2010

IMPACT FACTOR
2.753*
* As listed in the ISI® 2010 Science Citation Index Journal Citation Reports

OVER
500 000
full text downloads in 2010

30 DAYS
average receipt to online publication in 2010

16 961
citations in 2010
37% increase from 2007

"We've had a very positive experience with EPL, and not only on this occasion. The fact that one can identify an appropriate editor, and the editor is an active scientist in the field, makes a huge difference."

Dr. Ivar Martinv
Los Alamos National Laboratory, USA

Six good reasons to publish with EPL

We want to work with you to help gain recognition for your high-quality work through worldwide visibility and high citations.

1. **Quality** – The 40+ Co-Editors, who are experts in their fields, oversee the entire peer-review process, from selection of the referees to making all final acceptance decisions
2. **Impact Factor** – The 2010 Impact Factor is 2.753; your work will be in the right place to be cited by your peers
3. **Speed of processing** – We aim to provide you with a quick and efficient service; the median time from acceptance to online publication is 30 days
4. **High visibility** – All articles are free to read for 30 days from online publication date
5. **International reach** – Over 2,000 institutions have access to EPL, enabling your work to be read by your peers in 100 countries
6. **Open Access** – Articles are offered open access for a one-off author payment

Details on preparing, submitting and tracking the progress of your manuscript from submission to acceptance are available on the EPL submission website **www.epletters.net**.

If you would like further information about our author service or EPL in general, please visit **www.epljournal.org** or e-mail us at **info@epljournal.org**.

EPL is published in partnership with:

European Physical Society | Società Italiana di Fisica | EDP Sciences | IOP Publishing

A Letters Journal Exploring the Frontiers of Physics

March 2012

EPL, **97** (2012) 56005 www.epljournal.org
doi: 10.1209/0295-5075/97/56005

Different water scenarios for a primitive model with two types of hydrogen bonds

Yusong Tu[1,2,3], Sergey V. Buldyrev[2,4], Zengrong Liu[2,5], Haiping Fang[1,3] and H. Eugene Stanley[2]

[1] *Institute of Systems Biology, Shanghai University - Shanghai, 200444, China*
[2] *Center for Polymer Studies, Physics Department, Boston University - Boston, MA, 02215, USA*
[3] *Shanghai Institute of Applied Physics, Chinese Academy of Sciences - Shanghai, 201800, China*
[4] *Department of Physics, Yeshiva University - New York, NY, 10033, USA*
[5] *Department of Mathematics, Shanghai University - Shanghai, 200444, China*

received 4 November 2011; accepted in final form 6 February 2012
published online 6 March 2012

PACS 64.70.Ja – Liquid-liquid transitions
PACS 61.20.Ja – Computer simulation of liquid structure
PACS 61.20.Gy – Theory and models of liquid structure

Abstract – Using a primitive water model, we find that the strength of tetrahedral interactions can change the behavior of liquid water from the liquid-liquid critical point scenario to the singularity-free scenario. Specifically, we find that the strongly tetrahedral model has a liquid-liquid critical point from which the Widom line emanates with a negative slope, but that the weakly tetrahedral model lacks the second critical point and the line of the specific heat maxima analogous to the Widom line has a positive slope. The strongly tetrahedral interaction is characterized by a double-step potential that depends on hydrogen-bond bending, while the weakly tetrahedral interaction has a uniform single-step potential.

When water is cooled, its thermodynamic response functions, *e.g.*, specific heat C_P, isothermal compressibility K_T, and thermal expansivity $-\alpha_P$, dramatically increase. Theorists have proposed several interpretations for these low-temperature anomalies in liquid water, including the stability limit scenario [1], the liquid-liquid critical point (LLCP) scenario [2], and the singularity-free scenario [3]. Theoretical models of the hydrogen-bond (H-bond) interactions with different cooperativity have been designed to support one or more of these scenarios [4–6]. Very recently a Hamiltonian lattice model was proposed which can reproduce all the above scenarios by tuning the parameter of H-bond cooperativity strength [7].

The increase of C_P upon cooling is weak in molecular simulations of TIP3P and SPC-E water models but is more pronounced in TIP5P and ST2 models [2,8], which have stronger tetrahedrality. Moreover, the TIP5P and ST2 models clearly display a first-order liquid-liquid phase transition (LLPT) at low temperatures [9,10], while the TIP3P and SPC-E do not. The discrepancy between these water models in computational simulations is not well understood, and it is still unclear how the details of molecular bonding affect the behavior of real water in the deeply supercooled region of its phase diagram.

To explore the relationship between water anomalies and H-bond interactions, we adopt a coarse-grained model for H-bond tetrahedral orientation [11,12]. We expand the complex H-bond interactions by a zeroth-order approximation of a broad angular well (weakly tetrahedral), which corresponds to the orientations of distorted and weak H-bonds, and a first-order approximation of an additional narrow angular well (strongly tetrahedral), which corresponds to the orientations of linear H-bonds caused by strong electrostatic interactions between protons and lone pairs. Eisenberg and Kauzmann used a well-defined angular region of the energy curve to describe "distorted" H-bonds [13]. The question of how the potential energy of H-bonds depends on their distortion is still unclear and under debate [13–17].

Preliminary results [12] suggest that a strongly tetrahedral model reproduces the thermodynamic properties of liquid water, including both the anomalies at ambient temperatures and the LLCP at low temperatures indicated by the divergence of C_P and K_T. By systematically studying both strongly and weakly tetrahedral models over a broad range of pressures and temperatures, we find that weakening tetrahedrality of H-bonds may change the behavior from the LLCP scenario to the singularity-free

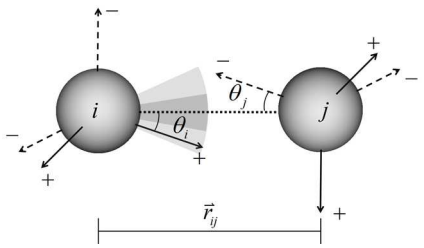

Fig. 1: The sketch of interaction potential in strong tetrahedrality model. Two water molecules are modeled by two hard-spheres with indices i and j separated by a distance r_{ij}. Each molecule consists of a hard sphere of a diameter σ with four arms pointing to the corners of a tetrahedron. A sign is associated with each of the four arms, two positives and two negatives, respectively, representing two hydrogen atoms and the oxygen lone electronic pair.

scenario. Specifically, in the strongly tetrahedral model the LLCP and the negatively sloped Widom line are enclosed in the region of the density anomaly, while the weakly tetrahedral model follows the singularity-free scenario in which the C_P maxima line has a positive slope and is located above the region of the density anomaly as in the Jagla model [18,19].

Figure 1 shows a schematic diagram of a strongly tetrahedral model in which water molecules are represented by three-dimensional hard spheres of diameter σ with four tetrahedrally-oriented arms [12]. In each molecule ($i = 1, 2, \ldots, N$) two arms represent protons and have positive signs ($s(i) = 1$), and two represent lone pairs and have negative signs ($s(i) = -1$). Neighboring water molecules i and j can form H-bonds via a discontinuous interaction potential that depends on the distance between the centers of the hard spheres r_{ij} and the angles between the arms and the radius vector connecting the centers of the spheres, θ_i and θ_j:

$$U_{ij}\left(r_{ij}, \theta_i, \theta_j\right) = \begin{cases} \infty, & r_{ij} < \sigma, \\ s(i)s(j)\varepsilon_{\mathrm{sHB}}, & \sigma \leqslant r_{ij} < f\sigma \text{ and} \\ & |\theta_i| < \theta_s \text{ and } |\theta_j| < \theta_s, \\ s(i)s(j)\varepsilon_{\mathrm{wHB}}, & \sigma \leqslant r_{ij} < f\sigma \text{ and} \\ & |\theta_i| < \theta_w \text{ and } |\theta_j| < \theta_w \\ & \text{and } (|\theta_i| \geqslant \theta_s \text{ or } |\theta_j| \geqslant \theta_s), \\ 0, & \text{otherwise}, \end{cases} \tag{1}$$

where f is a well-width parameter and $\varepsilon_{\mathrm{sHB}}$ and $\varepsilon_{\mathrm{wHB}}$ are, respectively, the energies of strongly tetrahedral and weakly tetrahedral H-bonds. The angles θ_i and θ_j are the smallest of the four angles between the arms of the molecules i and j, respectively, and the line connecting their centers. The molecules do not interact if $r_{ij} > f\sigma$ or if at least one particle lacks arms within the lightly or heavily shaded area. Strong H-bonds ($\varepsilon_{\mathrm{sHB}}$) form, when both arms lie in the heavily shaded region ($|\theta_i| < \theta_s$ and $|\theta_j| < \theta_s$), and they orient the four neighboring water molecules in a nearly perfect tetrahedron. Weak H-bonds ($\varepsilon_{\mathrm{wHB}}$) form, either when both arms lie in the light-shaded regions or when one arm lies in the light-shaded region and the other one in the dark-shaded one ($|\theta_i| < \theta_w$ and $|\theta_j| < \theta_w$ and ($|\theta_i| \geqslant \theta_s$ or $|\theta_j| \geqslant \theta_s$)), and they cause a widespread deviation from tetrahedral orientation among the molecules. Throughout the paper we use σ and $\varepsilon_{\mathrm{sHB}}$ as units of length and energy, respectively. We measure temperature T in units of $\varepsilon_{\mathrm{sHB}}/K_{\mathrm{B}}$, where K_{B} is the Boltzmann constant. The unit of pressure P is $\varepsilon_{\mathrm{sHB}}/\sigma^3$, and the unit of density ρ is σ^{-3}.

In principle, potentials with more than two steps can be introduced and treated as higher-order approximations of hydrogen-bond interaction. Here, we use the weakly tetrahedral model with only one step ($f = 1.1$, $\varepsilon_{\mathrm{HB}} = \varepsilon_{\mathrm{sHB}} = \varepsilon_{\mathrm{wHB}} = 1$, and $\theta_m = \theta_s = \theta_w = 27^\circ$) introduced by Bol [11] (the weakly tetrahedral model does not have the narrow dark shaded area and the particles interact with energy $\varepsilon_{\mathrm{HB}}$ if $r_{ij} \leqslant f\sigma$ and both molecules have arms in the light shaded area, see fig. 1), and the strongly tetrahedral model with two steps ($f = 1.1$, $\varepsilon_{\mathrm{sHB}} = 1$, $\varepsilon_{\mathrm{wHB}} = 0.68$, and $\theta_s = 12^\circ$, $\theta_w = 27^\circ$) [12]. Together with the Bol model, a family of simple ("primitive") models has been proposed [20] that uses hard-sphere repulsion and directional attraction, and that includes patchy particle models [21–23]. All these models consider only constant-interaction strength. Here we demonstrate the importance of including the angular dependence of the potentials in order to increase the H-bond strength for conformations with a higher tetrahedral order.

We obtain our results using Monte Carlo (MC) simulations, employing an aggregation-volume-bias algorithm and a configurational-bias method with multiple orientations [24,25]. These methods allow us to circumvent the bottleneck of the Metropolis algorithm at low temperatures, in which the acceptance rates of the configurations with higher energies are extremely low. The configurational bias we use allows a preference for configurations with higher entropies. However, even using these advanced MC techniques, very long MC runs are necessary to equilibrate the system at low temperatures (see ref. [12]). We discard the first 1×10^7 MC steps to allow the system to equilibrate, and then collect statistics from the next 1×10^7 MC steps. We use Verlet neighbor lists [26] to speed up the search for interacting pairs. Thermal properties, such as C_P, α_P, and K_T, are obtained in the isobaric (NPT) ensemble, and the system state points are calculated in the isochoric (NVT) ensemble [12]. Unless otherwise specified, system size N is set at 300. We also simulate systems with $N = 1000$ and results are consistent within the error bars. Ensemble averages are performed over 40 independent runs of each state point.

Figure 2 shows the pressure along isotherms and isochores. When the tetrahedrality is strong, a "flat" isotherm develops at the lowest studied temperature $T = 0.1$ (see fig. 2(a) and its inset). The presence of this flat region indicates divergent compressibility,

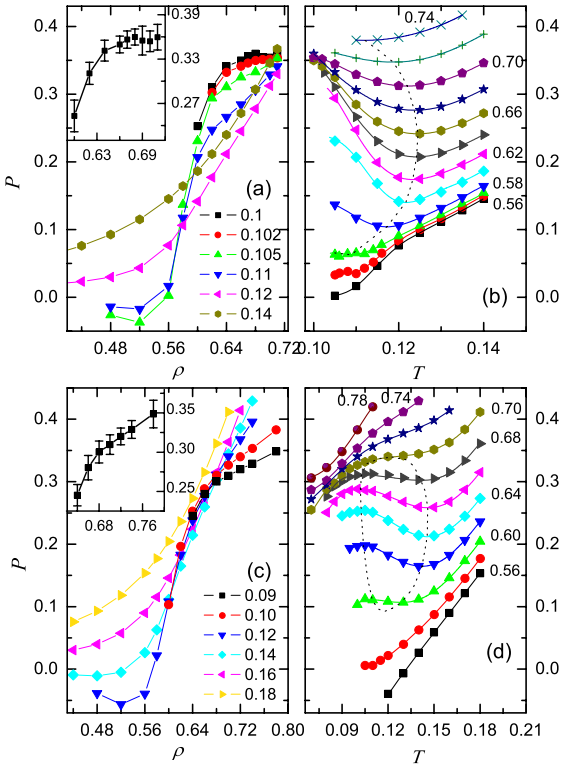

Fig. 2: (Colour on-line) Comparison of the equations of state of the strongly tetrahedral model ((a) and (b)), and the weakly tetrahedral model ((c) and (d)). Panels (a) and (c) show isotherms on the ρ-P plane, and numbers behind symbols indicate temperatures. Panels (b) and (d) show isochores on the T-P plane, numbers close to curves indicate densities of isochores, the solid curves are obtained by polynomial fit, and the dashed lines are lines of ρ maxima and minima bounding the density anomaly region. Insets on the ρ-P planes show the lowest-temperature isotherms: $T=0.1$ in (a) and $T=0.09$ in (c).

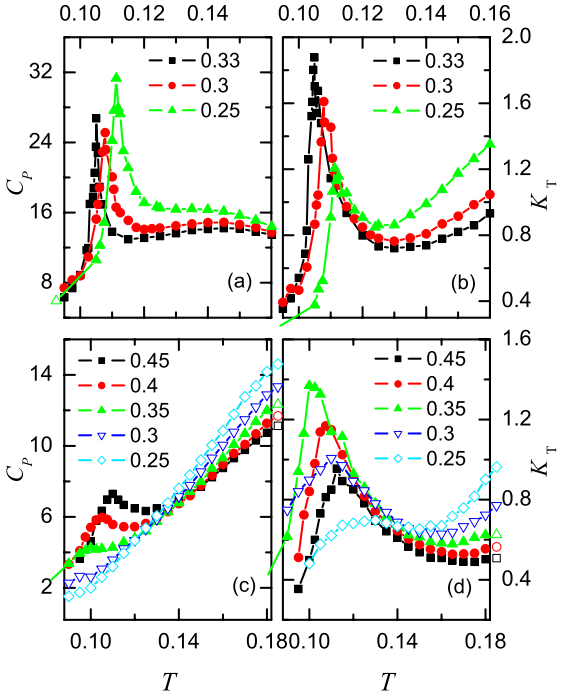

Fig. 3: (Colour on-line) Behavior of thermodynamic response functions for the models of strong (a), (b) and weak (c), (d) tetrahedrality. Isobaric temperature dependence of C_P (a), (c) and K_T (b), (d). The numbers indicate the pressure.

associated with the LLCP, which we estimate to be at $P_C = 0.36 \pm 0.015$, $T_C = 0.1 \pm 0.003$, and $\rho_C = 0.68 \pm 0.03$.

This LLCP estimation is based on the study of the shapes of the isotherms. We use the well-known condition for the critical point: $(\partial P/\partial\rho)_T = (\partial^2 P/\partial\rho^2)_T = 0$ [27,28]. The large error bars in the LLCP estimation are due to the fact that the inflection points of the isotherms are located at $\rho \approx 0.68$ while the system spontaneously crystallizes at $\rho \approx 0.72$. Also we were able to find only one subcritical isotherm $T = 0.99$ with a region of negative compressibility. Below this temperature we are not able to equilibrate the system due to the slowing-down of MC dynamics near the glass transition. Thus, our estimate of the critical point lies very close to the border of the region accessible by MC simulations and hence is not accurate.

The presence of a density anomaly is indicated by the crossing of the isotherms, and the region of density anomaly is defined by ρ maxima and minima, which are indicated by the minima and maxima of the isochores, respectively, since $(\partial P/\partial T)_V = \alpha_P/K_T = 0$. It is clear that the temperature of maximum density (TMD) changes its slope from negative to positive as P decreases, and that the lines of maximal and minimal density converge and join at $\rho \approx 0.57$. This is the point that indicates the minimal pressure at which the density anomaly exists. The TIP5P and ST2 water models have a similar scenario [9,10,27].

In contrast, in the weakly tetrahedral model all the isotherms have positive slopes, compressibility does not diverge, and no LLCP is present. An elliptically shaped region of density anomaly is bounded by the line of ρ minima that joins the line of ρ maxima not only at low pressures but also at high pressures.

We next study thermodynamic response functions C_P and K_T, which are computed from the fluctuations of energy and volume, respectively, in NPT ensembles. We find that both models display C_P maxima (figs. 3(a) and (c)). In the strongly tetrahedral model, C_P maxima become sharper as P increases and shift to lower T on approaching LLCP (fig. 3(a)). Note that the area under the C_P peak decreases as we approach LLCP. This phenomena is due to an anomalous increase of entropy with pressure in the low-density liquid (LDL), which follows from the density anomaly via a Maxwell relation. Thus, the difference between the entropies of the high-density liquid (HDL) and the LDL decreases as we approach LLCP. We cannot observe the compressibility and specific-heat maxima at $P > P_c$ because the system crystallizes at low temperatures [29]. In the weakly

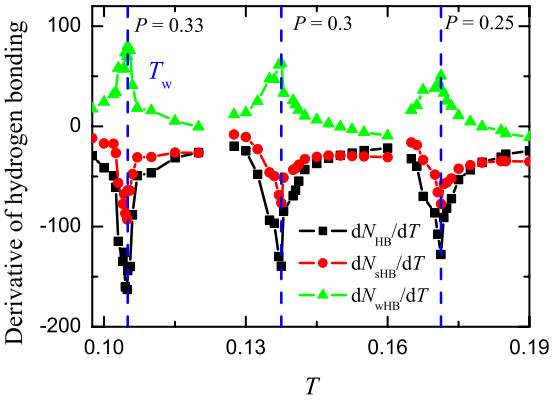

Fig. 4: (Colour on-line) Temperature derivatives of the number of different types of H-bonds numbers per molecule (strong, $N_{\rm sHB}$, weak, $N_{\rm wHB}$, and sum, $N_{\rm HB} = N_{\rm sHB} + N_{\rm wHB}$) in the model of strong tetrahedrality for several constant pressures. Vertical dashed lines indicate the temperatures of C_P maxima. Curves for $P = 0.3$ and 0.25 are shifted for clarity to high T, respectively by 0.03 and 0.06.

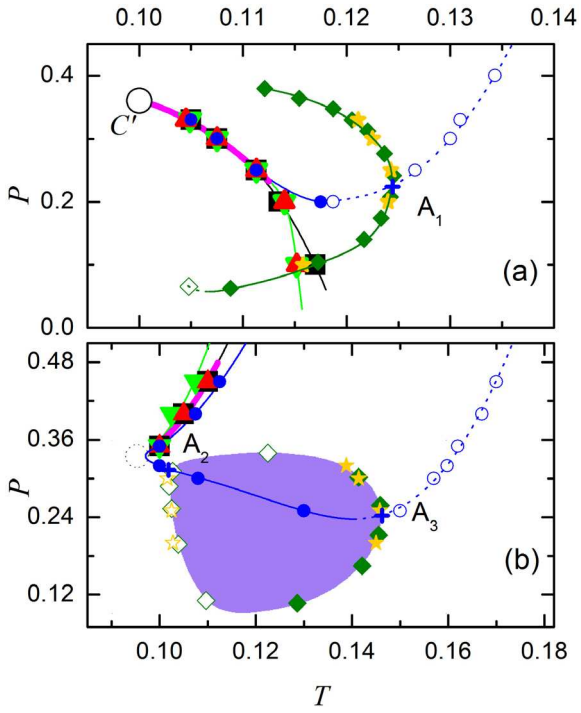

Fig. 5: (Colour on-line) The parts of the P-T phase diagrams showing density anomaly regions in (a) strong tetrahedrality model and (b) weak tetrahedrality model. On the plane P-T, we show the loci of ρ maxima (♦, ⋆) and minima (◇, ⋆), the loci of K_T maxima (●) and minima (○), the loci of $|\alpha_P|$ maxima (▲), the loci of C_P maxima (■), and the loci of $|\partial N_{\rm HB}/\partial T|_P$ maxima (▼) (see footnote [1]). The circle C' in (a) indicates the LLCP, and the big dotted circle in (b) indicates the position of the global K_T maximum. All curves are a guide to the eyes, with the solid thin curve representing the maxima of relevant quantities and the dashed thin lines representing the minima. A purple heavy curve represents the Widom line $T_{\rm w}(P)$ in (a) or its analogue in (b) which is drawn through the first three C_P maxima. A_1, A_2 and A_3 are the crossing points between the lines of K_T and ρ extremes.

tetrahedral model, C_P maximum can be observed only for $P > 0.35$, above the region of density anomaly (fig. 3(c)). But as the pressure decreases, the maximum does not diverge —it becomes weaker and disappears when $P < 0.35$.

At the same time, both models display K_T maxima and minima (figs. 3(b) and (d)). In the strongly tetrahedral model, K_T maxima increase and become sharper, and shift to lower T as P approaches P_C at which K_T seems to diverge (fig. 3(b)). In the weakly tetrahedral model, K_T does not diverge and does not lead to a critical point, but exhibits a global maximum at $P = 0.35$, $T = 0.1$. Note that as P increases above 0.35 or decreases below 0.35 the values of K_T maxima decrease gradually (fig. 3(d)).

To better understand the behavior of C_P, we study the role of two types of H-bonds in the strongly tetrahedral model. We find that the temperature derivatives of H-bond numbers display strong maxima and minima (fig. 4), which occur at the temperatures coincident with C_P maxima for the same pressures (fig. 3(a)). These derivative extremes indicate the state points at which there is the greatest exchange of strong and weak H-bonds in response to changes in temperature. The strong H-bonds are responsible for the highly ordered LDL local structure, and the weak H-bonds are responsible for the disordered HDL local structure, and this competition between the two local structures causes the C_P maxima. Note that these extremes become sharper as P increases and approaches the LLCP.

Figure 5(a) shows the phase diagram of the strongly tetrahedral model. The lines of maximal C_P, K_T, and $|\alpha_P|$, converge toward the Widom line $T_{\rm w}(P)$ with a negative slope and then approach the C' LLCP. This is consistent with experiments [30,31] and simulations using more complex water models, such as TIP4P/2005, TIP5P and ST2 [9,10,27,28]. The increase of C_P in water is related to the structural changes in the liquid. The strongly tetrahedral model provides a clear illustration of this relationship. We find that the locus of $|\partial N_{\rm HB}/\partial T|_P$ maxima coincides with the Widom line $T_{\rm w}(P)$ [12], which is consistent with predictions from the theoretical Hamiltonian lattice model [32]. Note that the loca of $|\partial N_{\rm sHB}/\partial T|_P$, $|\partial N_{\rm wHB}/\partial T|_P$, $|\partial N_{\rm HB}/\partial T|_P$ coincide with one another (fig. 4). This suggests that above the Widom line (for $T > T_{\rm w}(P)$), when weak H-bonds dominate the liquid, it becomes less structured and has a higher density, while below the Widom line (for $T < T_{\rm w}(P)$), when strong H-bonds dominate the liquid, it becomes more structured

[1] All data are computed directly from NPT simulations, except for the ρ data with diamond symbols that are estimate from extremes of the isochores in fig. 2 computed in NVT ensembles. The coincident results in both ensembles demonstrate the accuracy of our simulations. Also, the crossing of the lines of ρ and K_T extremes shows the agreement with theoretical analyses by Sastry *et al.* [3] and the simulation results of ST2 water model [9].

and has a lower density. When the liquid crosses the Widom line it thus exhibits the maximal rate of structural change in response to temperature change. This maximum provides direct evidence that HDL and LDL structures compete along the Widom line, and that this competition may evolve into a separation of the two phases at temperatures below the LLCP.

Note that the critical point does not exist in the weakly tetrahedral model. K_T reaches its global maximum within the dotted circle on the P-T plane (figs. 5(b) and 3(d)), but does not diverge. One can see two branches of K_T maxima emanating from this global maximum. The lower branch has a negative slope and crosses the region enclosed by the lines of minimal and maximal density. The upper branch is located above the density anomaly region, is nearly coincident with the lines of C_P and $|\alpha_P|$ maxima, and produces a line with a positive slope. Similarly, the Jagla model also exhibits a K_T maxima with two branches, the upper one with a positive slope that emanates from its critical point and asymptotically coincides with the Widom line [18,19]. Hence, in the weakly tetrahedral model, this positively sloped line can be considered an analogue to the Widom line in the singularity-free scenario but, because the C_P maxima fade away, no critical point forms (see fig. 3(c)). The line of K_T maxima turns on the P-T plane without a divergence in compressibility.

The behavior of the thermodynamic response functions in water at ambient conditions is consistent with both the singularity free scenario realized in the weakly tetrahedral model and the LLCP scenario realized in the strongly tetrahedral model. The existence of the LLCP depends on the mechanism of hydrogen-bond bending and on a strong competition between the weak (distorted) H-bonds abundant in HDL and the strong (linear) H-bonds abundant in LDL. This competition is made clear in our strongly tetrahedral model in which the configurations with the H-bonds created by the second (narrow and deep) attractive well have lower energy and entropy than the configurations with H-bonds created by the first (broad and shallow) attractive well. Thus, these two configurations may, within a certain temperature range, have the same Gibbs free energies and thus may coexist as LDL and HDL.

If we remove this broad and shallow well and leave only the strong narrow well ($f = 1.1$, $\varepsilon_{\rm HB} = \varepsilon_{\rm sHB} = \varepsilon_{\rm wHB} = 1$, $\theta_m = \theta_s = \theta_w = 12^\circ$), our system spontaneously crystallizes at $T \approx 0.125$ far above the expected location of the LLCP. Indeed, models of patchy tetrahedral interaction with a single well [23,29] suggest that the increase of rigidity of tetrahedral interactions increases crystallization temperature. The effects of both the patch angular width and the interaction range (corresponding to, respectively, θ_m and f in the weakly tetrahedral model) on glass formation and glass-crystal competition have been discussed in detail in refs. [23,29]. However, no LLPT has been observed in these models. We hypothesize that this is because only a single-step potential well has been adopted in these models. We conclude that the angular dependence of the strength of tetrahedral interactions is the key factor for the existence of LLPT. Varying the strength of strong and weak hydrogen bonds in our model one will be able to explore the criteria for the existence of the liquid-liquid phase transition in supercooled water and other tetrahedral liquids such as silicon.

* * *

This work was supported by IPSHMEC (11YZ20), NNSFC (10832006,10825520,11105088), KIP of CAS and the Shanghai Supercomputer Center of China. SVB acknowledges the partial support of this research through the Dr. Bernard W. Gamson Computational Science Center at Yeshiva College. HES thanks the NSF Chemistry Division (grants CHE 0911389 and CHE 0908218) for support.

REFERENCES

[1] Speedy R. J., *J. Phys. Chem.*, **86** (1982) 3002.
[2] Poole P. H., Sciortino F., Essmann U. and Stanley H. E., *Nature*, **360** (1992) 324.
[3] Sastry S., Debenedetti P. G., Sciortino F. and Stanley H. E., *Phys. Rev. E*, **53** (1996) 6144; Stanley H. E., *J. Phys. A*, **12** (1979) L329; Stanley H. E. and Teixeira J., *J. Chem. Phys.*, **73** (1980) 3404.
[4] Poole P. H., Sciortino F., Grande T., Stanley H. E. and Angell C. A., *Phys. Rev. Lett.*, **73** (1994) 1632.
[5] Borick S. S., Debenedetti P. G. and Sastry S., *J. Phys. Chem.*, **99** (1995) 3781.
[6] Tanaka H., *Europhys. Lett.*, **50** (2000) 340.
[7] Stokely K., Mazza M. G., Stanley H. E. and Franzese G., *Proc. Natl. Acad. Sci. U.S.A.*, **107** (2010) 1301.
[8] Brovchenko I., Geiger A. and Oleinikova A., *J. Chem. Phys.*, **123** (2005) 044515.
[9] Poole P. H., Saika-Voivod I. and Sciortino F., *J. Phys.: Condens. Matter*, **17** (2005) L431.
[10] Paschek D., *Phys. Rev. Lett.*, **94** (2005) 217802.
[11] Bol W., *Mol. Phys.*, **45** (1982) 605.
[12] Tu Y. and Fang H., *Phys. Rev. E*, **79** (2009) 016707.
[13] Eisenberg D. and Kauzmann W., *The Structure and Properties of Water* (Oxford University Press, New York) 1969.
[14] Smith J. D., Cappa C. D., Wilson K. R., Cohen R. C., Geissler P. L. and Saykally R. J., *Proc. Natl. Acad. Sci. U.S.A.*, **102** (2005) 14171.
[15] Auer B. M. and Skinner J. L., *J. Chem. Phys.*, **128** (2008) 224511.
[16] Huang C., Wikfeldt K. T., Tokushima T., Nordlund D., Harada Y., Bergmann U., Niebuhr M., Weiss T. M., Horikawa Y., Leetmaa M., Ljungberg M. P., Takahashi O., Lenz A., Ojamäe L., Lyubartsev A. P., Shin S., Pettersson L. G. M. and Nilsson A., *Proc. Natl. Acad. Sci. U.S.A.*, **106** (2009) 15214.

[17] Clark G. N. I., Cappa C. D., Smith J. D., Saykally R. J. and Head-Gordon T., *Mol. Phys.*, **108** (2010) 1415.
[18] Xu L., Buldyrev S. V., Angell C. A. and Stanley H. E., *Phys. Rev. E*, **74** (2006) 031108.
[19] Buldyrev S. V., Malescio G., Angell C., Giovambattista N., Prestipino S., Saija F., Stanley H. and Xu L., *J. Phys.: Condens. Matter*, **21** (2009) 504106.
[20] Nezbeda I. and Slovak J., *Mol. Phys.*, **90** (1997) 353.
[21] Kern N. and Frenkel D., *J. Chem. Phys.*, **118** (2003) 9882.
[22] Bianchi E., Largo J., Tartaglia P., Zaccarelli E. and Sciortino F., *Phys. Rev. Lett.*, **97** (2006) 168301.
[23] Romano F., Sanz E. and Sciortino F., *J. Chem. Phys.*, **132** (2010) 184501.
[24] Siepmann J. I. and Frenkel D., *Mol. Phys.*, **75** (1992) 59.
[25] Chen B. and Siepmann J. I., *J. Phys. Chem. B*, **105** (2001) 11275.
[26] Verlet L., *Phys. Rev.*, **159** (1967) 98.
[27] Yamada M., Mossa S., Stanley H. E. and Sciortino F., *Phys. Rev. Lett.*, **88** (2002) 195701.
[28] Abascal J. L. F. and Vega C., *J. Chem. Phys.*, **133** (2010) 234502; **134** (2011) 186101.
[29] Romano F., Sanz E. and Sciortino F., *J. Chem. Phys.*, **134** (2011) 174502.
[30] D'Arrigo G., Maisano G., Mallamace F., Migliardo P. and Wanderlingh F., *J. Chem. Phys.*, **75** (1981) 4264.
[31] Angell C. A. and Rodgers V., *J. Chem. Phys.*, **80** (1984) 6245.
[32] Kumar P., Franzese G. and Stanley H. E., *Phys. Rev. Lett.*, **100** (2008) 105701.